

A century of glacier change in the Wind River Range, WY



Mark H. DeVisser^{a,b,*}, Andrew G. Fountain^{a,b}

^a Department of Geology, Portland State University, Portland, OR 97207, USA

^b Department of Geography, Portland State University, Portland, OR 97207, USA

ARTICLE INFO

Article history:

Received 22 July 2013

Received in revised form 26 September 2014

Accepted 11 October 2014

Available online 24 October 2014

Keywords:

Glaciers

Perennial snow and ice

Wind River Range, WY

Climate change

ABSTRACT

The Wind River Range spans roughly 200 km along the continental divide in western Wyoming and encompasses at least 269 glaciers and perennial snowfields totaling $34.34 \pm 0.13 \text{ km}^2$ (2006), including Gannett Glacier, the largest glacier (2.81 km^2) in the continental U.S. outside of Washington State. To track changing glacier and perennial snow surface area over the past century we used historic maps, aerial photography, and geologic evidence evident in said imagery. Since the end of the Little Ice Age (~1900), when the glaciers retreated from their moraines, to 2006 the ice-covered area shrank by ~47%. The main driver of surface area change was air temperature, with glaciers at lower elevations shrinking faster than those at higher elevations. The total contribution of ice wastage to late summer stream flow ranged from 0.4 to 1.5%, 0.9 to 2.8%, 1.7 to 5.4%, and 3.4 to 10.9% in four different watersheds, none of which exceeded 7% glacier cover. Results from previous studies were difficult to include because of differences in interpretation of glacier boundaries, because of poor imagery, or to extensive seasonal snow. These difficulties highlight potential problems in combining data sets from different studies and underscores the importance of reexamining past observations to ensure consistent interpretation.

© 2014 Elsevier B.V. All rights reserved.

1. Introduction

Interest in global glacier shrinkage has increased in recent decades owing to its consequences for sea level rise (Dyurgerov and Meier, 2000; Kaser et al., 2006; Pfeffer et al., 2008) and loss of water storage capacity (Jansson et al., 2003; Barnett et al., 2005). Regionally, perennial ice and snow are important to the hydrology of high alpine environments (e.g., Moore et al., 2009), with meltwater buffering stream flow during warm dry summers (Fountain and Tangborn, 1985; Moore et al., 2009). Improved inventories of ice-covered regions and assessments of glacier change are needed to better quantify these estimates and to inform on past and possible future contributions to the hydrologic cycle.

Perennial ice and snow in the Wind River Range are of particular interest because of important runoff contributions to the Green–Colorado, Missouri–Mississippi, and Snake–Columbia basins (Marston et al., 1989, 1991). Runoff into the Missouri River basin is especially important to eastern Wyoming as a vital water source during the dry summer months and years of low precipitation (Pochop et al., 1989). The need for water in Wyoming is demonstrated by the 2006 state-funded weather modification project (\$8.8 million USD) to increase

winter snowfall with the intention of increasing snowmelt runoff during the summer (Boe, 2008). Therefore, assessing temporal and spatial patterns of glacier wastage in the Wind River Range is important for understanding stream flow variation in the region. The purpose of this paper is to present a comprehensive inventory of glaciers and perennial snowfields (G&PS) in the Wind River Range, quantify their area changes over the twentieth century, identify the factors influencing the changes, and estimate the volume loss and its contribution to regional runoff.

2. Background

The Wind River Range spans roughly 200 km along the continental divide in western Wyoming. Based on 1:24,000 U.S. Geological Survey topographic maps, the Range contains 679 G&PS (Fountain et al., 2007), with a combined surface area of about 55.8 km^2 (Fig. 1). The region contains 25 of Wyoming's 38 named glaciers, including Gannett Glacier, the largest glacier in the continental U.S. outside of Washington State (Pochop et al., 1990). The earliest documented exploration of the Wind River Range was John Fremont's expedition of 1841 that included climbing the peak that now bears his name (Sprague, 1964). In 1877 the U.S. Geological and Geographical Survey of the Territories, otherwise known as the Hayden Survey, arrived in the Wind River Range to catalog the geology, biology, and geography (Hayden, 1878). However, no glaciers were observed because of the persistence of seasonal snow late into the summer (Hayden, 1879). The survey returned to the region in 1878 and,

* Corresponding author at: Department of Geography, Michigan State University, East Lansing, MI 48824, USA. Tel.: +1 517 432 9238.

E-mail address: devisse6@msu.edu (M.H. DeVisser).

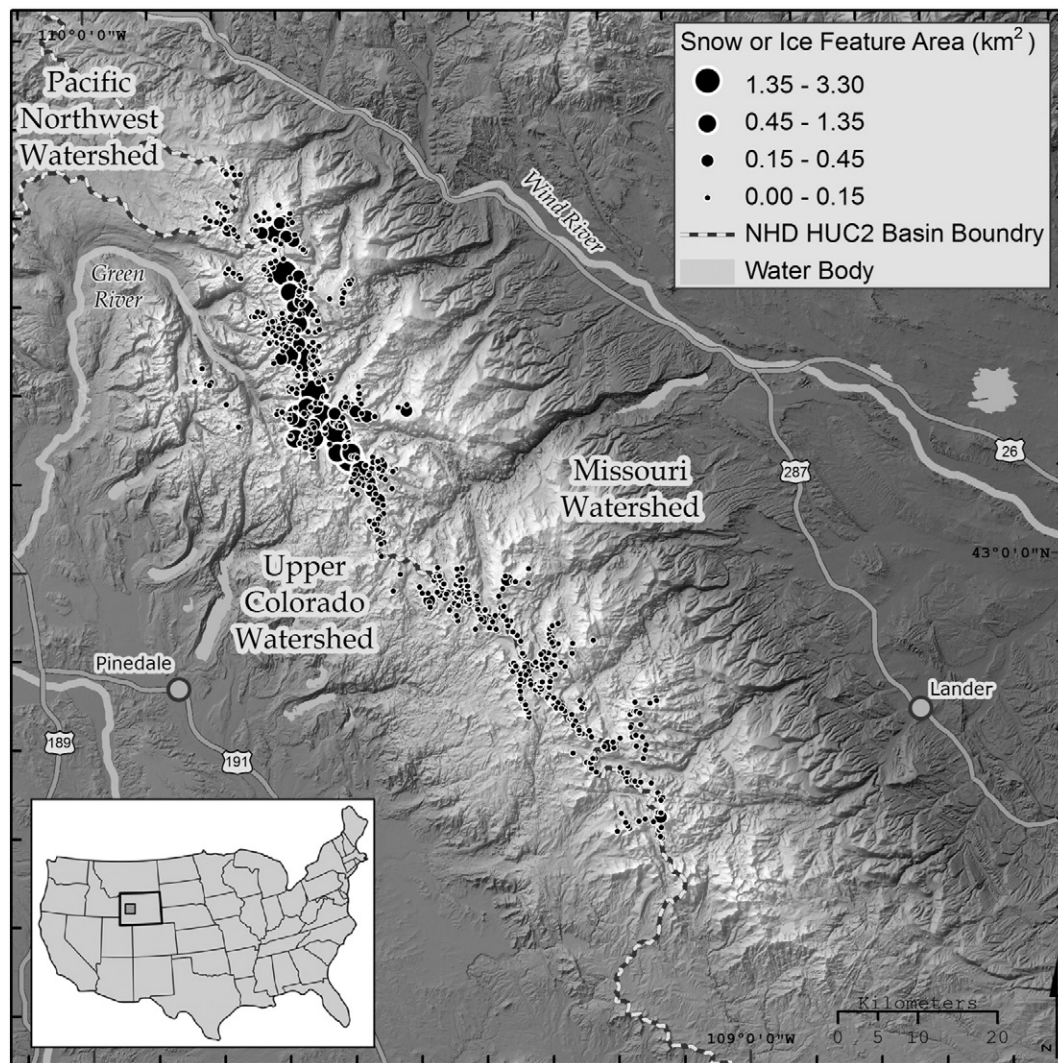


Fig. 1. Location of the Wind River Range in western Wyoming and of the 679 snow and ice features identified on USGS 24K topographic maps by Fountain et al. (2007). Note that snow and ice features are not to scale.

because of the relatively low snowfall the previous winter and subsequent earlier exposure of glacial ice (Russell, 1885), made the first recorded observation of glaciers on the north side of Wind River peak (Hayden, 1878). Subsequent glacier discoveries around Fremont peak were made soon after (Hayden, 1883).

The first topographic maps that depicted glaciers were limited to the area around Fremont peak and completed in 1906 by the U.S. Geological Survey (USGS) (Wilson, 1907). Unfortunately, the glacial outlines are generalized precluding their use for area estimates (Meier, 1951). The first published scientific investigation of the glaciers examined the North, East, and West Gannett Glaciers, now referred to as Gannett, Dinwoody, and Mammoth glaciers, respectively, and included approximate measurements of surface area (Wentworth and Delo, 1931). Delo returned to Dinwoody Glacier in 1940 to observe ‘the extensive recession of the glaciers during the intervening decade,’ but no measurements were reported (Delo, 1940). The first application of modern glaciological methods was completed by Meier (1951), concentrating on the region around Gannett and Fremont peaks. He constructed detailed maps of 14 named glaciers and included the Little Ice Age (LIA) maximum extent and the 1950 extent. Results showed that all glaciers examined

were receding with losses between 7 and 41% of their LIA maximum. Since that time, a number of studies documented continued glacier shrinkage (Marston et al., 1989, 1991; Wolken, 2000; Cheesbrough, 2007; Thompson et al., 2011; VanLooy et al., 2014). The mean retreat rate of Dinwoody Glacier was 5.4 m year^{-1} and for Gannett Glacier 8 m year^{-1} between 1958 and 1983 (Marston et al., 1989, 1991). Dinwoody lost 36.9% (1.28 km^2) from 1950 to 1999 (Wolken, 2000), or 39.7% (1.44 km^2) of its LIA area. The area change of 42 glaciers from 1985 to 2005 was -37% (Cheesbrough, 2007). Over this time period, runoff from glacial mass loss during the July–October period was estimated to contribute 4.7–9.8% of the runoff in various watersheds (Cheesbrough, 2007). Unfortunately, no mass balance measurements have been recorded in this region.

Our effort differs from these previous reports in several ways. First, we compile a comprehensive inventory of not only glaciers, defined as perennial snow or ice that moves (Cuffey and Paterson, 2010), but we also attempt to inventory the perennial snowfields as well. Second, we examine all the publicly available fine resolution imagery to develop a time series of glacier change for the entire population of G&PS. Third, we incorporate the results from all previous studies to develop a detailed history of glacier change for the subset

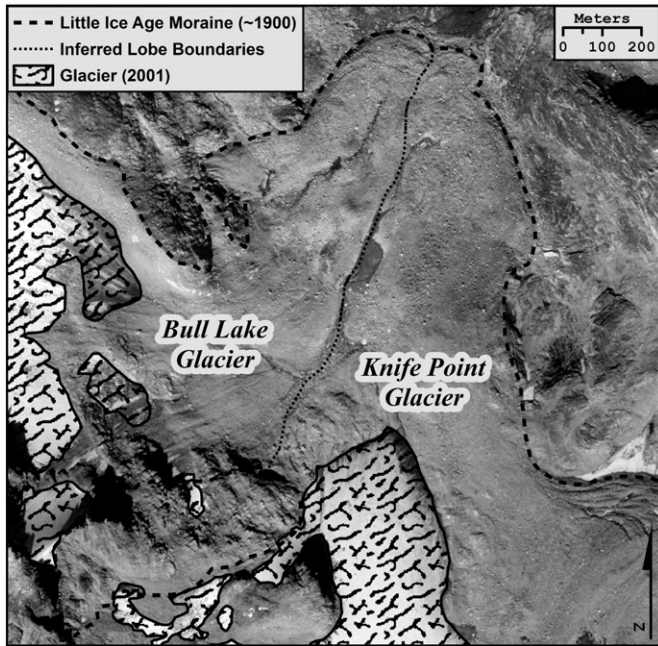


Fig. 2. Visible Little Ice Age moraines on Bull Lake and Knife Point glaciers, Wind River Range, on the 2001 digital orthographic photograph from Sanborn Colorado LLC. The moraines were delineated using Meier's (1951) maps as a guide, and lobe boundaries were separated based on inferred ice flow divides.

of glaciers with a rich data legacy, from which we infer glacier change for the entire Range. Finally, we examine these results to define the climate drivers and impact on regional hydrology.

3. Methods

3.1. Glaciers and perennial snowfields

We compiled the perimeter and surface areas of G&PS digitized from various maps and aerial photos because they are the most spatially and temporally extensive data available. The USGS 1:24,000 topographic (24K) maps provided the baseline coverage for the location, perimeter, and surface area of G&PS features. The 24K maps were based on aerial photos acquired in the summers of

1966, 1968, 1974, and 1989; each including 76%, 2%, 14%, and 8% of the total number of G&PS, respectively.

To assess glacier change we digitized the perimeter of all visible snow and ice present in digital orthophotograph quadrangle (DOQ) imagery acquired from the Wyoming Geographic Information Science Center (WyGIS), University of Wyoming, and the National Agriculture Imagery Program (NAIP). All of the DOQs had a spatial resolution of 1 m and were acquired during late summer in 1994 (black-and-white) and in 2001, 2006, and 2009 (color). Late summer photography minimizes the confounding effects of seasonal snow. Unfortunately, despite the late summer acquisition, the 2009 DOQs showed a snowy alpine landscape, and we excluded the imagery from our analysis. However, Dinwoody Glacier was relatively unaffected by the seasonal snow, and we were able to clearly identify and digitize the perimeter, allowing us to include the 2009 surface area. We did not use satellite imagery because of either the prohibitive cost or inappropriate spatial resolution given the size of the G&PS features in the region (Thompson et al., 2011).

One challenge we faced is the definition of perennial snow. Unlike glaciers, which are typically easy to identify because of the exposure of ice, distinguishing seasonal from perennial snow is somewhat ambiguous. We define seasonal features as those that have the potential to melt completely in the summer months of any given year. However, because our study is based solely on remotely sensed imagery acquired at erratic intervals, we have limited means to track changes in these features. Seasonal features may appear in multiple years of imagery caused by persistent patterns of snow accumulation. Depending on regional climate patterns and local influences of avalanches, wind redistribution, and terrain shadowing, some seasonal features may even survive multiple summers before completely melting away again. To standardize our interpretation of seasonal versus perennial, we adopted four interpretation rules. First, any feature found in the photography that was not included in the 24K, were assumed to be seasonal (and ignored). Second, 24K features that were not found in the 1994 photography were considered seasonal. Third, 24K features that were found in the 1994 photography but not in the 2001 and 2006 photography were assumed to be perennial features that disappeared. Fourth, if a feature is present on multiple images but exhibits a standard deviation of area >40% of the 24K area, then it was considered too affected by seasonal snow and excluded from the analysis. The threshold of 40% was empirically determined by identifying the smallest ratio associated with features that flickered between presence/absence in the time series of the imagery. This approach defines perennial as features that are present for 20+ years. Results from these interpretation rules showed that only small features, typically <0.1 km², were affected.

The G&PS inventory is partitioned into glaciers and perennial snowfields. If ground observations were available, including direct measurements and presence of crevasses or fine-grained sediment in the glacial streams (evidence of basal sliding), we could distinguish between the two features by movement (Cuffey and Paterson, 2010). Because our study is entirely based on maps and remotely sensed imagery, we cannot detect movement directly, and we did not inspect the images for crevasses. Instead, movement was inferred based on whether the calculated basal shear stress exceeded the yield stress of ice (Basagic and Fountain, 2011). The basal shear stress is calculated from the thickness and surface slope of the ice and the yield stress, 10⁵ Pa (Cuffey and Paterson, 2010). Thickness is estimated from the glacier volume (see below) divided by the measured surface area. Surface slope is the maximum slope, derived from the 1 arc sec National Elevation Dataset (NED) digital elevation model (DEM) (Fountain et al., 2007). Topography is limited to the 24K data set, and we used the glacier area from the 24K for consistency.

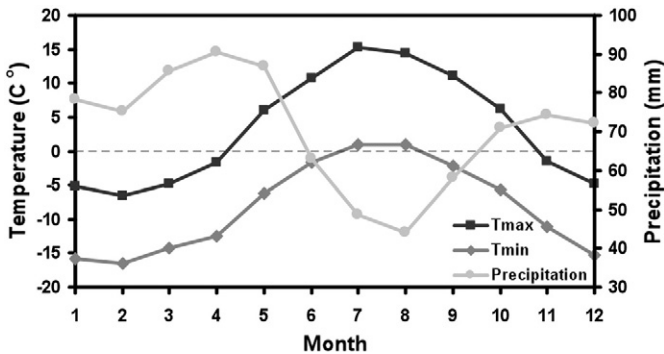


Fig. 3. Mean monthly maximum temperature (Tmax), minimum temperature (Tmin), and precipitation for the study region calculated from PRISM data. The dotted line indicates 0 °C.

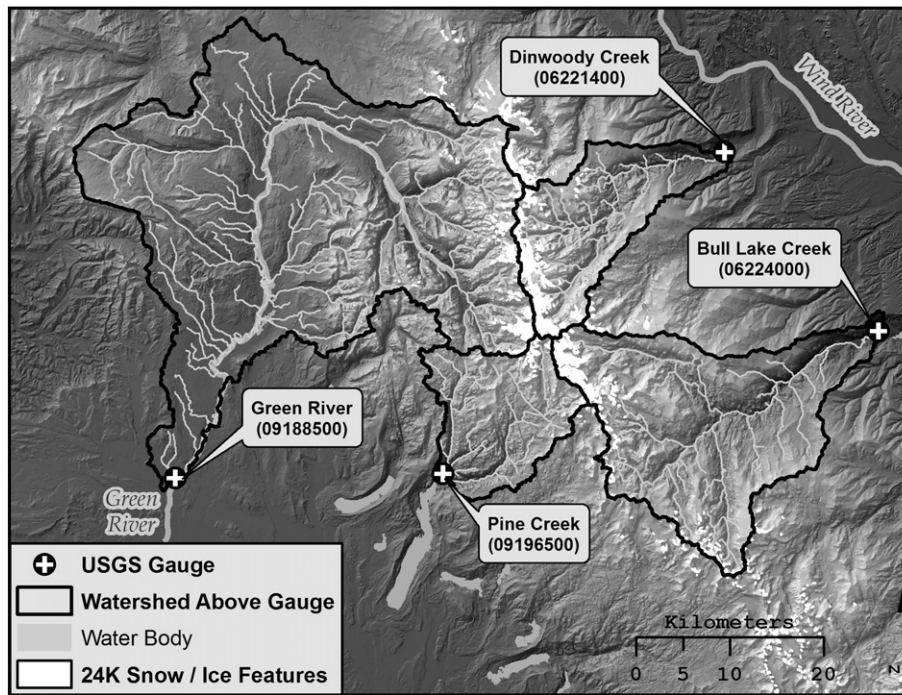


Fig. 4. The four USGS gauge stations and upstream watershed in relation to the snow and ice features identified in the 24K maps. Note, snow and ice features are not to scale.

In addition to the regionwide inventories of G&PS, a number of individual glaciers have been studied over numerous years, providing greater insight on historic changes. Meier (1951) produced 14 maps of glaciers, derived from unorthorectified aerial photos and field observations, which included a 1950 perimeter and the LIA maximum extent. Each of Meier's maps were individually scanned and georeferenced to the 2001 DOQs within ArcGIS. At least 11 control points were used, along with a third order transformation, which provided the best fit between the maps and DOQs. Owing to the remote location of the Wind River Range, hard ground control points (e.g., roads, building corners) were absent, forcing us to rely on soft ground control points (e.g., terminal moraines, headwalls, nunataks) (Hughes et al., 2006). Of the 14 glacier maps, 12 were successfully georeferenced, then digitized within ArcGIS. Two glaciers, Sphinx and F-3, could not be georeferenced because of the lack of suitable ground control. Another two glaciers, Fremont and Knife Point have split and have been officially renamed since the Meier study. Fremont Glacier is now the Upper Fremont and Lower Fremont glaciers, and Knife Point is now Bull Lake and Knife Point glaciers.

While georeferencing the Meier (1951) maps, we realized that his mapped LIA extent served as an excellent guide to identifying LIA moraines that were easily observed on the 2001 DOQs (Fig. 2). Consequently, we were able to derive the LIA extents for eight additional glaciers not included in Meier (1951). Since the LIA, the glaciers have shrunk and retreated, and some lobes of the once larger glacier have separated into individual glaciers. For our analysis, we have separated the lobes into their modern analogues based on inferred ice flow divides (Fig. 2). The date associated with these LIA extents (i.e., the year the glacier retreated from the terminal moraine) was inferred to be ~1900, based on Wentworth and Delo (1931) who stated that 'it appears that there has been a moderate retreat of the glaciers and a restriction of glacial action in the last two decades in this district [Gannett Peak]'. Our inference is supported by historic photos of glacier change in the Sierra Nevada

Range, California, which showed the glaciers did not retreat from the LIA moraines before 1910 (Basagic and Fountain, 2011).

In addition to the LIA and 1950 measurements, Meier (1951) mapped the extent of Gannett Glacier in 1930 and 1940 from ground-based photography (Wentworth and Delo, 1931; Delo, 1940). Since 1950, Gannett and Dinwoody glaciers have been the targets of numerous glacier change studies (Marston et al., 1989; Pochop et al., 1989; Marston et al., 1991; Wolken, 2000) based on field surveys and on remotely sensed imagery from aircraft and satellites. Combining all of these supplementary surface area values allowed us to reconstruct surface area change for Gannett and Dinwoody in greater detail.

3.2. Uncertainty

Three main sources of uncertainty are encountered when defining the outline of G&PS: georectification, digitizing, and interpretation (DeBeer and Sharp, 2007; Sitts et al., 2010; Thompson et al., 2011). Georectification uncertainty refers to the quality of the imagery or maps being analyzed. Digitizing uncertainty represents the difference between the digitized boundary and the actual boundary of a feature (Gong et al., 1995). Interpretation uncertainty includes potential misinterpretation of a boundary leading to disagreement among multiple users' interpretations (Middelkoop, 1990). Interpretation uncertainty is often the largest of the three uncertainties because rock-covered ice, valley wall shadows, and seasonal snow can mask large areas (Pochop et al., 1989). Our rules of interpretation are in part an attempt to minimize interpretation uncertainty and dictate that only visible snow or ice is digitized. This approach may lead to underestimates of features masked by shadows or debris. Correspondingly, it's quite possible to misinterpret seasonal snow patches as perennial resulting in the overestimation of feature area. Interpretation error is difficult to quantify given that it has the potential to both overestimate and underestimate surface area, and it varies between users.

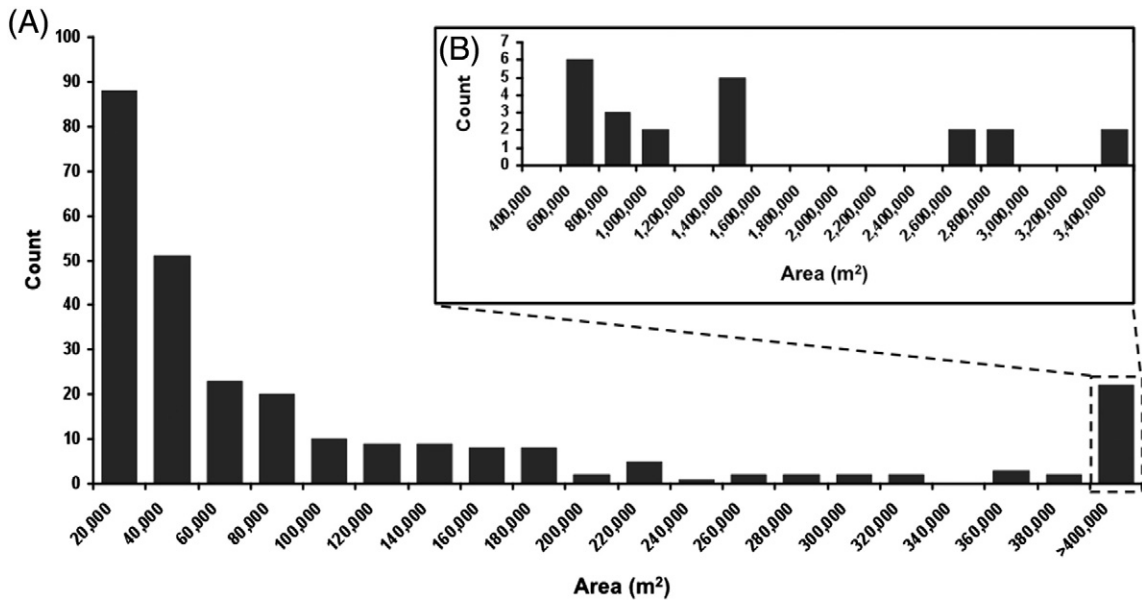


Fig. 5. The percent population of perennial features versus surface area. Note the scale change on X-axis between graphs A and B.

Digitizing and georectification uncertainty are closely linked. Digitizing error is dependent on the quality of the imagery and its spatial resolution relative to the size of the feature being digitized. The only published quality measure of the 24K maps and DOQs is positional accuracy associated with random uncorrelated points. However, polygon vertices are correlated and preclude positional uncertainty as an estimate of area uncertainty. To account for image quality and its impact on the user's ability to accurately digitize a boundary, we estimate a combined uncertainty of digitizing and georectification by multiplying the positional uncertainty (e.g., RMSE) by the spatial resolution of the image.

Uncertainty of features derived from the 24K maps was previously published by Fountain et al. (2007). To estimate the uncertainty in digitized features from the DOQs we adapted the uncertainty

calculation method used by Hoffman et al. (2007), based on Ghilani (2000), to incorporate the combined measure of digitizing and georectification uncertainty,

$$U = 1.414 * RMSE * R * A * \sqrt{2} \tag{1}$$

where U is the feature uncertainty (m^2), $RMSE$ is the root mean square error of the DOQs or georeferenced map (m), R is the spatial resolution of the imagery (m), and A is the surface area of the digitized feature (m^2).

The RMSE values used to estimate the uncertainty for each of the georeferenced Meier (1951) maps are calculated,

$$U_{Meier} = 1.414 * \sqrt{RMSE^2 + RMSE_{Georef}^2} * R * A * \sqrt{2} \tag{2}$$

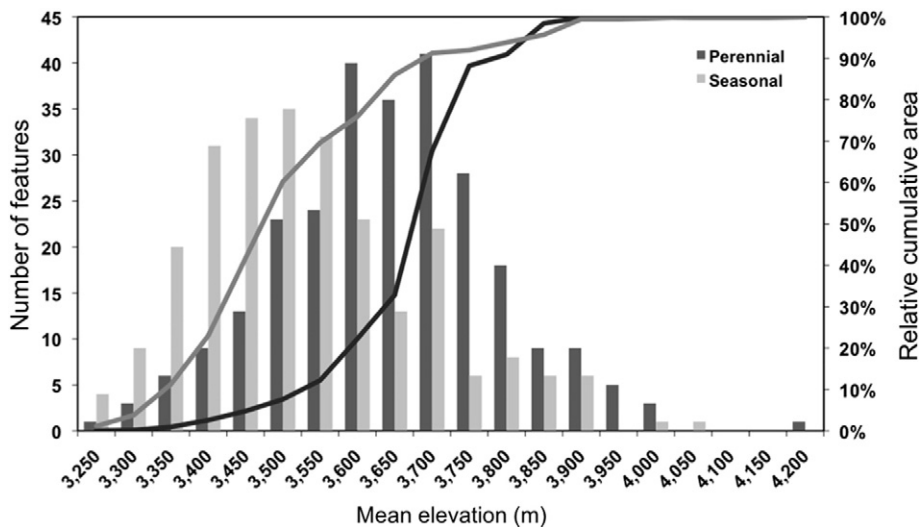


Fig. 6. The population versus centroid elevation of the 269 perennial and 251 seasonal features. Cumulative area is the total area of all features using 50m elevation bin intervals. Centroid elevation was derived from the 1 arc sec NED DEM.

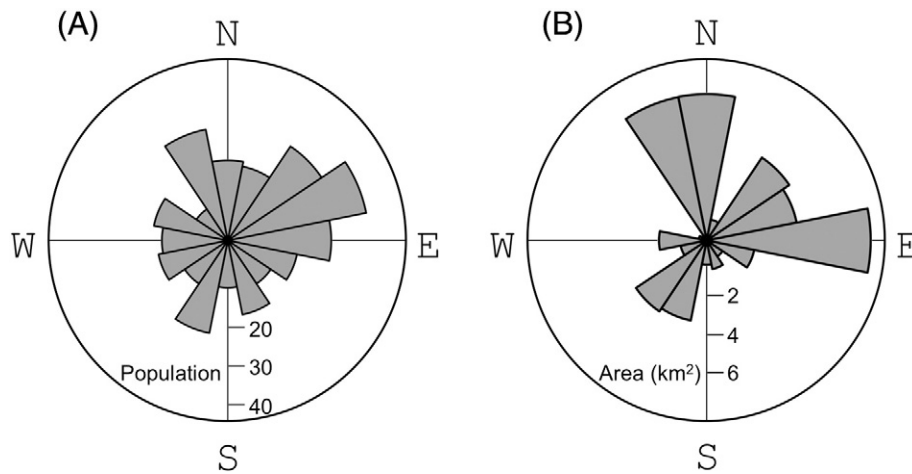


Fig. 7. Aspect of the 269 perennial snow and ice features in the Wind River Range: (A) distribution of the population of features in percent; (B) distribution of total ice-covered area (km²). The topographic characteristics are derived from digital elevation data based on aerial photography from 1963 to 1974.

where U_{Meier} is the feature uncertainty (m²), $RMSE$ is from the 2001 DOQs used for control points to georeference the Meier maps, $RMSE_{Georef}$ is the calculated RMSE produced from the georeferencing of the Meier maps (m), R is the spatial resolution of the 2001 DOQ (m), and A is the surface area of the digitized feature (m²).

3.3. Topographic and climate data

The topographic and climatic characteristics of the G&PS were extracted from the previously mentioned NED DEM and from gridded monthly air temperature and precipitation climate data. The DEM was used to derive the maximum, minimum, mean elevation, slope, and mean aspect for each G&PS (Fountain et al., 2007). We partitioned mean aspect into northness and eastness variables; with northness calculated by taking the cosine of the mean aspect, producing a value between 1 and -1 , with '1' being true north and -1 being true south. Eastness was calculated by taking the sine, with '1' being true east. No photogrammetric terrain data were included in the DOQs; consequently, we limited all topographic data, except area, to the 24K data set.

Monthly climate data were obtained from the 4-km gridded Parameter-elevation Regressions on Independent Slopes Model (PRISM) over the time period between 1900 and 2006 (Daly et al., 1997). The monthly data included total precipitation and mean,

minimum, and maximum air temperature. The 4-km grid cells are certainly much larger than the individual G&PS features. However, we are not interested in the specific climate of each feature but rather the surrounding region, and particularly, the temporal changes. Seasons were defined by mean monthly temperature calculated over the period of record: winter – both mean minimum and mean maximum monthly air temperatures were below 0 °C (November to April); spring and autumn – mean minimum temperature was below freezing and the mean maximum air temperature was above freezing (May and June, September and October); and summer – mean minimum and mean maximum temperatures were above 0 °C (July and August) (Fig. 3). To aggregate the monthly temperature data into seasonal time periods, we converted the data into degree-days above 0 °C and multiplied by the number of days in each month (Badescu and Zamfir, 1999). Although this method probably underestimates the number of degree-days (Wang et al., 2006), for our general purposes this approach is sufficient. We calculated degree-days for the mean maximum and for the mean minimum monthly air temperatures. Precipitation differences also followed the temperature-defined seasons, winter – greatest precipitation (~80 mm per month); and summer – the lowest precipitation (~45 mm per month). The monthly total precipitation and degree-days data were then summed for winter, spring, summer, and autumn periods.

Table 1

Area of 269 glaciers and perennial snowfields (G&PS) based on the USGS 1:24,000 (24K) maps and from aerial photographs^a.

24K date	Num	24K		1994			2001			2006		
		Area (km ²)	% U	Area (km ²)	% U	% change	Area (km ²)	% U	% change	Area (km ²)	% U	% change
1963	1	0.03	9.97	0.02	7.70	-44.8 ± 8.6	0.02	3.35	-45.0 ± 3.7	0.02	3.13	-38.60 ± 4.0
1966	217	43.70	0.26	37.83	0.16	-13.4 ± 0.4	33.21	0.07	-24.0 ± 0.1	32.33	0.07	-26.0 ± 0.1
	Avg.	0.20	2.67	0.17	1.61		0.15	0.71		0.15	0.73	
1968	5	0.53	2.38	0.36	1.65	-31.4 ± 2.4	0.30	0.78	-42.7 ± 0.9	0.38	0.69	-27.0 ± 1.1
	Avg.	0.11	4.82	0.07	3.22		0.06	1.45		0.08	1.29	
1974	46	2.71	1.05	1.66	0.77	-38.9 ± 1.0	1.20	0.39	-55.7 ± 0.3	1.61	0.33	-40.5 ± 0.4
	Avg.	0.06	6.42	0.04	4.44		0.03	2.21		0.04	1.96	
Total	269	46.96	0.25	39.86	0.16	-15.1 ± 0.4	34.73	0.07	-26.1 ± 0.1	34.34	0.07	-26.9 ± 0.1
	Avg.	0.17	2.92	0.15	1.74		0.13	0.77		0.13	0.80	

^a The 24K date is the year the aerial photographs were acquired to construct the 24K maps, and Num is the number of G&PS identified for that date. Area is the total area of G&PS for that year and U is its uncertainty. Change represents the change in total area from the 24K date. The average G&PS area and its uncertainty is provided for each data set.

Table 2

Reconstructed areas for 22 glaciers in the Wind River Range based on georeferenced maps (LIA, 1950) by Meier (1951) and on aerial imagery; the LIA inferred from aerial imagery (not from Meier, 1951) does not include data for 1950; LIA is Little Ice Age, U is the uncertainty in area.

Glacier name	LIA		1950		1966		1994		2001		2006	
	Area (km ²)	% U	Area (km ²)	% U	Area (km ²)	% U	Area (km ²)	% U	Area (km ²)	% U	Area (km ²)	% U
Baby Glacier	0.50	1.1	0.29	1.4	0.24	3.5	0.24	2.0	0.22	1.1	0.21	0.9
Bull Lake Glacier	2.04	0.7	1.44	0.8	1.36	1.5	1.33	0.9	1.28	0.4	1.21	0.4
Connie Glacier	0.59	1.4			0.46	2.6	0.39	1.6	0.34	0.9	0.33	0.7
Dinwoody Glacier	3.63	0.6	3.17	0.6	3.06	1.0	2.65	0.6	2.43	0.3	2.38	0.3
Downs Glacier	1.00	1.1			0.61	2.2	0.54	1.3	0.55	0.7	0.51	0.6
Gannett Glacier	5.25	0.5	4.01	0.6	3.32	0.9	3.01	0.6	2.90	0.3	2.81	0.3
Gooseneck Glacier	0.61	0.8	0.31	1.1	0.33	3.0	0.31	1.8	0.29	0.9	0.29	0.8
Grasshopper Glacier	4.16	0.5			3.28	1.0	2.79	0.6	2.46	0.3	2.34	0.3
Harrower Glacier	0.40	1.7			0.22	3.7	0.21	2.1	0.18	1.2	0.16	1.1
Heap Steep Glacier	0.25	1.3	0.19	1.5	0.16	4.3	0.12	2.8	0.11	1.5	0.11	1.3
Helen Glacier	1.89	1.0	1.39	1.2	1.39	1.5	1.19	0.9	1.07	0.5	1.05	0.4
J Glacier	0.60	1.4			0.40	2.7	0.35	1.7	0.30	0.9	0.29	0.8
Knife Point Glacier	2.01	0.7	1.47	0.8	1.30	1.5	1.04	1.0	0.89	0.5	0.83	0.5
Lower Fremont Glacier	1.03	0.8	0.93	0.8	0.77	2.0	0.65	1.2	0.56	0.7	0.49	0.6
Mammoth Glacier	3.41	0.3	2.88	0.4	2.54	1.1	2.29	0.7	2.06	0.3	2.00	0.3
Minor Glacier	0.85	0.7	0.71	0.8	0.65	2.1	0.55	1.3	0.44	0.7	0.41	0.7
Sacagawea Glacier	3.64	0.7	3.18	0.8	3.28	1.0	2.38	0.6	2.10	0.3	2.11	0.3
Sourdough Glacier	1.64	0.8			1.33	1.5	1.11	0.9	1.02	0.5	0.99	0.4
Stroud Glacier	0.82	1.2			0.52	2.4	0.42	1.5	0.39	0.8	0.38	0.7
Tiny Glacier	0.04	5.1			0.03	10.1	0.03	6.0	0.02	3.3	0.02	3.0
Twins Glacier	0.79	1.0	0.58	1.1	0.49	2.5	0.35	1.7	0.32	0.9	0.27	0.8
Upper Fremont Glacier	1.52	0.7	1.33	0.7	1.23	1.4	1.28	0.8	1.26	0.4	1.21	0.4
Total	36.67	0.2			27.32	0.3	23.37	0.2	21.29	0.1	20.40	0.1
<i>Surface area change since LIA maximum extent</i>												
Fourteen Meier Glaciers	0.00%		-20.20%		-29.65%		-36.55%		-41.89%		-43.92%	
Eight Additional Glaciers	0.00%				-25.99%		-36.94%		-43.10%		-45.72%	

3.4. Correlation and principal component analysis

Pearson correlation coefficient and principal component analysis (PCA) were used to identify the climate and topographic variables that correlate with temporal changes in ice cover. The independent

variables for each G&PS included mean elevation, latitude, longitude, and aspect, and for the seasonal climate variables included precipitation, maximum temperature degree-days, and minimum temperature degree-days. Because the interval of time between area estimates was erratic, we summed the climate variables over the

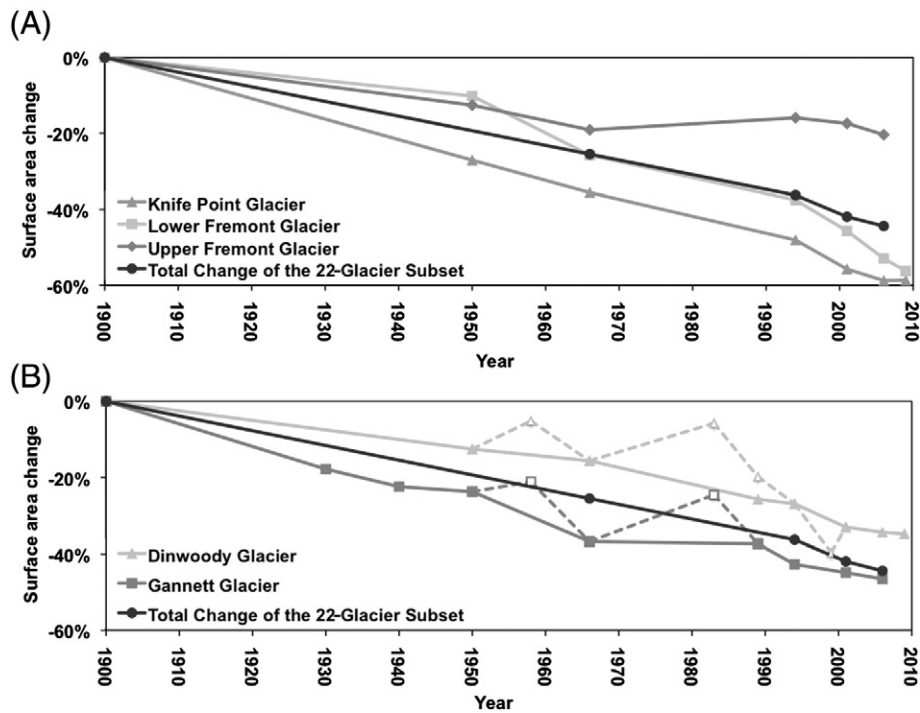


Fig. 8. Percent surface area change since the glacier's LIA maximum extent (i.e., ~1900) for (A) Knife Point, Lower Fremont, and Upper Fremont glaciers, and (B) Dinwoody and Gannett glaciers. Each graph also includes the combined total surface area change of all 22 glaciers that have identifiable LIA extents. The dotted lines for Dinwoody and Gannett glaciers represent the change in surface area when the areas obtained from Marston et al. (1989), Pochop et al. (1989), and Wolken (2000) are included.

Table 3
Surface areas, surface area uncertainty (*U*), and area change relative to the LIA extent for Gannett and Dinwoody glaciers ('na' indicates no data).

		1900	1930	1940	1950	1966	1989	1994	2001	2006	2009
Gannett	Area (km ²)	5.25	4.32	4.08	4.01	3.32	3.29	3.01	2.90	2.81	na
	<i>U</i> (km ²)	±0.03	±0.02	±0.02	±0.02	±0.03	na	±0.02	±0.01	±0.01	
	% change	0.0	−17.8	−22.4	−23.7	−36.8	−37.3	−42.7	−44.9	−46.5	
Dinwoody	Area (km ²)	3.63	na	na	3.17	3.06	2.70	2.65	2.43	2.38	2.37
	<i>U</i> (km ²)	±0.02			±0.02	±0.03	na	±0.02	±0.01	±0.01	±0.01
	% change	0.0			−12.5	−15.6	−25.7	−26.9	−33.0	−34.3	−34.7

interval. For example, if the interval between aerial photographs was 10 years, then the winter precipitation and degree-days for each season was summed for that 10-year period.

Significant relationships were identified using a one-tailed 95% confidence interval for the Pearson correlation analysis. The predicted relationship between surface area change and a given variable used in the analysis can be viewed in [Table A1](#). We used the PCA to aggregate correlated variables from 1966 to 2006 into uncorrelated classes (i.e., factors) and then identify which factors have the greatest variance between individual G&PS. The PCA was performed using Varimax rotation and a significant loading threshold of ≥ 0.7 to identify the pertinent variables in each factor. The number of factors extracted from the PCA was chosen by examining the eigenvalues, explained variance, scree plot, and an introduced random variable, which was used to identify the break point between viable factors and background noise inherently present in the data.

3.5. Ice mass wastage contribution to runoff

To estimate the contribution of ice wastage to stream flow, ice volume loss is compared to measured runoff. Glacier volume was estimated for two different times based on scaling relations between glacier area and volume ([Granshaw and Fountain, 2006](#); [DeBeer and Sharp, 2007](#); [Marks, 2012](#)) and using a bulk ice density for glacier ice of 880 kg m^{−3} ([LaChapelle, 1965](#)). Two relations were applied, one theoretical ([Bahr et al., 1997](#)) and one empirical ([Chen and Ohmura, 1990](#)). Both equations take the form,

$$V = bA^c \quad (3)$$

where, *V* is the ice volume, *A* is the ice area, and *b* and *c* are constants. For the theoretical relation, *b* = 0.90 and *c* = 1.396 ([Bahr et al., 1997](#)) and for the empirical, *b* = 28.50 and *c* = 1.396 ([Chen and Ohmura, 1990](#)). Estimates of glacier volume in the Wind River Range using [Bahr et al. \(1997\)](#) were found to provide adequate, if underestimated, estimates of glacier volume change ([Marks, 2012](#)). However, we recognize that the relation between area change and volume change is not necessarily consistent across all glaciers (e.g., [VanLooy et al., 2014](#)). In addition, Eq. (3) results in significant errors for individual G&PS. To compensate for high individual feature

Table 4
Estimate of total perennial ice-covered area for the Wind River Range (asterisk (*) indicates estimates from the 14 Meier (1950) glaciers).

Year	14 Meier glaciers area (km ²)	217 G&PS area (km ²)
LIA	27.42	67.77*
1950	21.88	51.29*
1966	19.29	43.7
1994	17.40	37.83
2001	15.93	33.21
2006	15.38	32.33

uncertainty, G&PS volumes are summed for each watershed ([Granshaw and Fountain, 2006](#)), and reported as a range of volumes estimates using [Chen and Ohmura \(1990\)](#) and [Bahr et al. \(1997\)](#) as the maximum and minimum values, respectively.

Daily mean stream flow data were obtained from four USGS gauge stations, Bull Lake Creek (station number – 06224000), Dinwoody Creek (06221400), Green River (09188500), and Pine Creek (09196500) ([Fig. 4](#)). However, approximately year-long gaps in recorded stream flow data occurred for each station. To fill the data gaps, we identified the neighboring gauge station whose stream flow best correlated with the gauge of interest, then linear regression was used to fill in the gaps. To prevent spurious values being produced from the gap-filling process (e.g., negative stream flow values), the regression results were bounded by the minimum and maximum stream flow values ever recorded at the gauge station for the particular day being filled. The watershed upstream of each gauging station was delineated using the ArcHydro extension in ArcGIS 9.2 using the 1 arc sec DEM and following the methods outlined in [Maidment \(2002\)](#); defining the stream gauge location as the outlet, or in GIS terms, pour point. The centroid of each G&PS was used to identify which basin meltwater drained. We assume that ice melt (mass loss from long-term storage) only occurs from August to September when seasonal snow extent is a minimum and glacier ice/perennial snow is most exposed. We also assume that all melt becomes runoff with no loss to evaporation or to groundwater.

4. Results and analysis

A total of 679 snow and ice features were found on the 24K maps with a combined area of 54.59 ± 0.13 km² ([Table A2](#)). We were unable to accurately digitize outlines for 159 features in either the 1994, 2001, or 2006 imagery, owing to shadows or late season snowfall; hence these features were removed from our analysis. The 24K area of the removed features totaled 3.55 km², with an average and median area of 0.02 km². Based on our rules of interpretation, 251 features were identified as seasonal and removed from the analysis, totaling 4.08 km², with an average area of 0.02 km² and median of 0.01 km². A total of 269 G&PS were identified with combined area of 46.96 ± 0.12 km², a mean area of 0.175 km², and a median of 0.037 km² ([Fig. 5A](#)). Of these G&PS, 43 (16%) were identified as glaciers based on their basal shear stress, and they represented 74% of the G&PS area. The mean centroid elevation of the G&PS ranges from 3239 m to 4153 m, averaging 3651 m ([Fig. 6](#)). No preferred aspect exists for the number of G&PS, but the total area is greatest facing north and east, indicating larger features, as expected for the Northern Hemisphere ([Fig. 7](#)).

Comprehensive inventories of the 269 G&PS were compiled for the 24K (spanning 1963–1974), 1994, 2001, and 2006 ([Table 1](#)). During this time the ice-covered area shrank by 26.9% to 34.34 ± 0.13 km². We further partitioned the G&PS data set based on the dates associated with 24K quadrangles to examine glacier change ([Table 1](#)). Although we believe that the G&PS changed little over

Table 5

Results of the Pearson correlation analysis showing the significant correlations (95% level) between area change of glaciers and perennial snowfields, and climate and topographic variables for each time period. Two data sets are examined, the 217-glacier and perennial snowfields and the 14 glaciers that have the longest and most complete data record. NA indicates the lack of statistical significance.

Surface area data set	Highest significant correlated variable			
	Positive		Negative	
Time period	Variable	Correlation coefficient	Variable	Correlation coefficient
<i>All perennial features</i>				
1966–1994	Mean elevation	0.51	Winter maximum temperature	−0.35
1966–2001	Maximum elevation	0.50	Winter maximum temperature	−0.25
1966–2006	Mean elevation	0.35	Winter maximum temperature	−0.26
1994–2001	Maximum elevation	0.21	NA	
<i>Glacier subset</i>				
1900–1966	Maximum elevation	0.44	NA	
1900–1994	Mean elevation	0.64	NA	
1900–2001	Mean elevation	0.74	NA	
1900–2006	Mean elevation	0.74	NA	
1966–1994	Mean elevation	0.49	NA	
1966–2001	Mean elevation	0.58	NA	
1966–2006	Mean elevation	0.61	NA	
1994–2001	Mean elevation	0.39	NA	
1994–2006	Maximum elevation	0.58	Autumn maximum temperature	−0.41
2001–2006	Maximum elevation	0.55	Spring maximum temperature	−0.52

the 11-year period of imagery acquisition, to ensure absolute temporal consistency, our analysis of change was limited to a subset of 217 features obtained from quadrangles with a 1966 acquisition date. In 1966, the 217 G&PS covered an area of $43.70 \pm 0.11 \text{ km}^2$, 78% of the total ice-covered area, averaging 0.201 km^2 . Over the 40-year period from 1966 to 2006, the total ice-covered area decreased by 26% to $32.33 \pm 0.02 \text{ km}^2$ at a rate of $-0.28 \text{ km}^2 \text{ year}^{-1}$. The median area decreased from 0.036 km^2 to 0.023 km^2 . The fastest rate of change was from 1994 to 2001, $-0.66 \text{ km}^2 \text{ year}^{-1}$; whereas the other two periods, 1966–1994 and 2001–2006, were about $-0.2 \text{ km}^2 \text{ year}^{-1}$. We are unable to detect G&PS disappearance prior to 1994 because

of our interpretation rules, but no G&PS was observed to disappear since 1994.

4.1. Change since the Little Ice Age

Meier (1951) maps provided the LIA and 1950 extent for 14 glaciers, 1930 and 1940 extents for Gannett Glacier, and allowed us to infer the LIA extents for eight other glaciers. We georeferenced the Meier (1951) maps based on a balance between visual fit, the greatest number of GCP, and the lowest RMSE. The resulting RMSE was large, ranging between 0.7 and 6.7 m, resulting in higher uncertainty values. Our estimated glacier areas differed somewhat from that of Meier (1951), which we attribute to the georegistration of his otherwise unrectified maps, which supports Meier’s comments regarding the uncertainty associated with his maps. The revised LIA surface area measurements were generally smaller than those reported by Meier (1951), averaging -8.8% and ranging from -25% to $+12\%$; for the 1950 areas, -15% (-28% to $+1\%$). Our revised area estimates of Meier’s data were used to assess glacier change. Based on Meier’s mapping of the LIA extents, we could identify LIA moraines from the 2001 aerial imagery for eight other glaciers, bringing the total to 22 glaciers. Area changes since the LIA (~1900) to 2006 showed that over the last century the glaciers lost about 44% of their area (Table 2). Almost half of the change occurred in the past 35 years since 1966 (Fig. 8A).

Table 6

Principal component analysis of climate and topographic variables to explain the variance of the 217 glaciers and perennial snowfields over the period 1966–2006; significant loadings/factor coefficients (≥ 0.7) are labeled in bold.

Variable	Factor				
	1	2	3	4	5
	Elevation	Location	MinTemp	Precip	NA
Longitude	0.075	0.884	−0.028	0.267	0.098
Latitude	−0.107	− 0.942	0.145	0.133	−0.106
Minimum elevation	0.787	0.037	−0.020	−0.199	0.120
Maximum elevation	0.839	0.059	0.064	−0.108	−0.021
Mean elevation	0.949	0.015	0.024	−0.161	0.059
Northness	−0.031	0.151	0.160	0.068	0.499
Eastness	0.197	0.018	0.091	0.070	0.614
Min autumn temp	0.018	−0.089	− 0.908	0.150	−0.105
Min spring temp	0.032	0.295	− 0.912	0.150	−0.036
Min summer temp	−0.117	−0.045	− 0.897	0.291	−0.059
Max autumn temp	−0.367	0.433	−0.626	0.265	0.183
Max winter temp	−0.561	−0.390	−0.424	0.450	0.097
Max spring temp	−0.500	−0.348	−0.489	0.505	0.109
Max summer temp	−0.513	−0.475	−0.432	0.491	0.082
Autumn precipitation	0.276	0.145	0.167	− 0.923	−0.004
Winter precipitation	0.155	0.022	0.059	− 0.965	−0.002
Spring precipitation	0.256	−0.163	0.350	− 0.833	−0.020
Summer precipitation	0.072	−0.287	0.282	− 0.881	0.009
Random	0.080	0.031	0.220	0.135	−0.656
Eigenvalues	7.47	3.14	2.01	1.62	1.13
% variance explained	18.1	13.7	20.0	22.9	6.2

Table 7

USGS gauge watershed area, number of perennial snow and ice features, and feature area statistics; G&PS means glaciers and perennial snowfields, and % is the fraction of watershed covered in G&PS.

USGS gauge	Watershed area (km ²)	# of G&PS	G&PS area (km ²)			
			Total	%	Mean	Median
Bull Lake Creek	485	62	11.713	2.4	0.189	0.028
Dinwoody Creek	227	61	14.448	6.3	0.237	0.040
Green River	1202	47	7.956	0.7	0.169	0.020
Pine Creek	195	14	1.497	0.8	0.107	0.036

Table 8
Contribution of ice volume loss to the runoff from four watersheds in the Wind River Range^a.

Year		Watershed			
		Dinwoody Creek	Pine Creek	Green River	Bull Lake Creek
		Dinwoody Creek	Pine Creek	Green River	Bull Lake Creek
	1966 G&PS vol range (km ³)	0.499–0.158	0.024–0.008	0.220–0.070	0.340–0.107
	1994 G&PS vol range (km ³)	0.438–0.138	0.017–0.005	0.188–0.059	0.285–0.090
	2001 G&PS vol range (km ³)	0.381–0.120	0.014–0.004	0.157–0.049	0.250–0.079
	2006 G&PS vol range (km ³)	0.362–0.114	0.012–0.004	0.149–0.047	0.240–0.076
	Time period				
1966 to 1994	Vol change (km ³)	0.061–0.019	0.007–0.002	0.032–0.010	0.054–0.017
	Stream flow (km ³)	0.850	0.528	1.809	1.303
	% contribution	7.13–2.25	1.28–0.40	1.78–0.56	4.16–1.31
1994 to 2001	Vol change (km ³)	0.057–0.018	0.003–0.001	0.031–0.010	0.035–0.011
	Stream flow (km ³)	0.253	0.172	0.444	0.353
	% contribution	22.67–7.16	1.92–0.61	7.08–2.24	10.03–3.17
2001 to 2006	Vol change (km ³)	0.019–0.006	0.002–0.0005	0.007–0.002	0.010–0.003
	Stream flow (km ³)	0.153	0.057	0.221	0.163
	% contribution	12.66–4.00	2.67–0.84	3.30–1.04	6.04–1.91
Total	Vol change (km ³)	0.137–0.043	0.012–0.004	0.071–0.022	0.099–0.031
	Stream flow (km ³)	1.256	0.757	2.474	1.819
	% contribution	10.94–3.45	1.53–0.48	2.87–0.90	5.47–1.73

^a For each watershed the estimate range of G&PS volume for each inventory is provided with the total runoff for August and September for each time period of glacier volume change. USGS gauges for each watershed are Bull Lake Creek (USGS station number – 06224000), Dinwoody Creek (06221400), Green River (09188500), and Pine Creek (09196500).

Because Dinwoody and Gannett glaciers have been the focus of numerous glacier change studies over the years, we attempted to compile a more detailed history of area change by including data from these previous reports (Marston et al., 1991; Wolken, 2000; Cheesbrough, 2007). Unfortunately, data from Cheesbrough (2007) were inconsistent with our measurements and with the other authors for the three years reported in all studies (1989, 1994, and 1999) and we did not include them. This discrepancy is likely caused by the Landsat 5/7 satellite imagery used by Cheesbrough (2007), which has a relatively coarse spatial resolution of ~30 m when compared to the 1-m spatial resolution of the aerial photography (Thompson et al., 2011). The data for 1958, 1983, 1989, and 1999 from Marston et al. (1991) and Wolken (2000) were also inconsistent with our temporal trend of glacier area (Fig. 8B). By including their data, the area change was flashy, contrary to glacier behavior. To resolve the possible interpretation differences, we obtained copies of the aerial photographs for 1983 and 1989 used by Marston et al. (1991) and Wolken (2000). No 1958 photograph was found so we eliminated that year from our analysis. The 1983 aerial photograph revealed substantial seasonal snow precluding accurate area determination and was excluded from our analysis. The 1989 photograph exhibited little seasonal snow, and Dinwoody and Gannett glacier outlines were digitized following our rules of interpretation. For Dinwoody, we obtained a smaller (–7.2%) surface area than reported by Wolken (2000), which better matched the trend. The 1999 area of Dinwoody was mapped by Wolken (2000) using a hand-held GPS unit, but he reported limited access to the entire perimeter, therefore resulting in a smaller surface area. In total, we compiled seven area measurements for Dinwoody Glacier and nine for Gannett Glacier from ~1900 to 2006 (Table 3). The overall change of Dinwoody and Gannett glaciers from ~1900 to 2006 was –35% and –48%, respectively, and brackets the change of the 22 glaciers in the range of –46%. Over the last 40 years (1966–2006), the Dinwoody and Gannett glaciers each changed, relative to ~1900, about –11.2% and close to the average of –10.2% for the 22 glaciers.

Estimates of the changes of the total ice-covered area over the past century are derived by scaling the changes from the glacier subsets. The most robust measure of change is the 217 G&PS data

set because it accounts for 78% of the entire ice-covered area and because its topographic characteristics of the G&PS are not statistically different. However, estimating changes prior to 1966 requires utilizing the smaller glacier data sets (Table 2) composed of glaciers that are much larger than the typical G&PS of the region. To account for the differences between data sets, the total area for the 14 Meier (1951) glaciers and the 22-glacier data set were regressed against the total areas of the 217 data set over the period of overlapping data, 1966–1994. The regressions of both data sets resulted in correlation coefficients >0.99 and the regression using the total area of the 14 glaciers was slightly higher than that for the 22 glaciers. For that reason, and the fact that the 14 glacier record includes 1950, we used the 14-glacier subset regression equation to estimate the area change for the 217 glaciers prior to 1966 (Table 4).

4.2. Correlation and principal component analysis

The results of the correlation analysis showed overall physically reasonable results (Table 5; Table A1). Elevation exhibits the highest significant positive correlation coefficients for both data sets, the 217 G&PS and the 14 glaciers. That is, higher glaciers show less area loss than lower glaciers. For the climate variables, only maximum temperatures exhibited significant (negative) correlations. For the G&PS data set, maximum winter temperatures were significantly correlated over all periods including 1966–2006, except for 1994–2001. For the 14-glacier subset, maximum autumn air temperatures between 1994 and 2006 were significant, and for spring maximum temperatures, 2001–2006. Summer temperatures were not significant with either data set.

The PCA of the 217 G&PS resulted in four factors that explained ~75% of the variance (Table 6). In order of explained variance, precipitation (factor 4) explained ~23% of the variance with significant loadings (correlations) on all seasons; minimum temperature (factor 3), explained 20% of the variance with significant loadings on autumn, spring, and summer temperatures; elevation (factor 1) explained 18% of the variance, having significant loadings on all three elevation variables; and latitude/longitude or location (factor 2) explained 13.7% of the variance. The elevation loadings support the

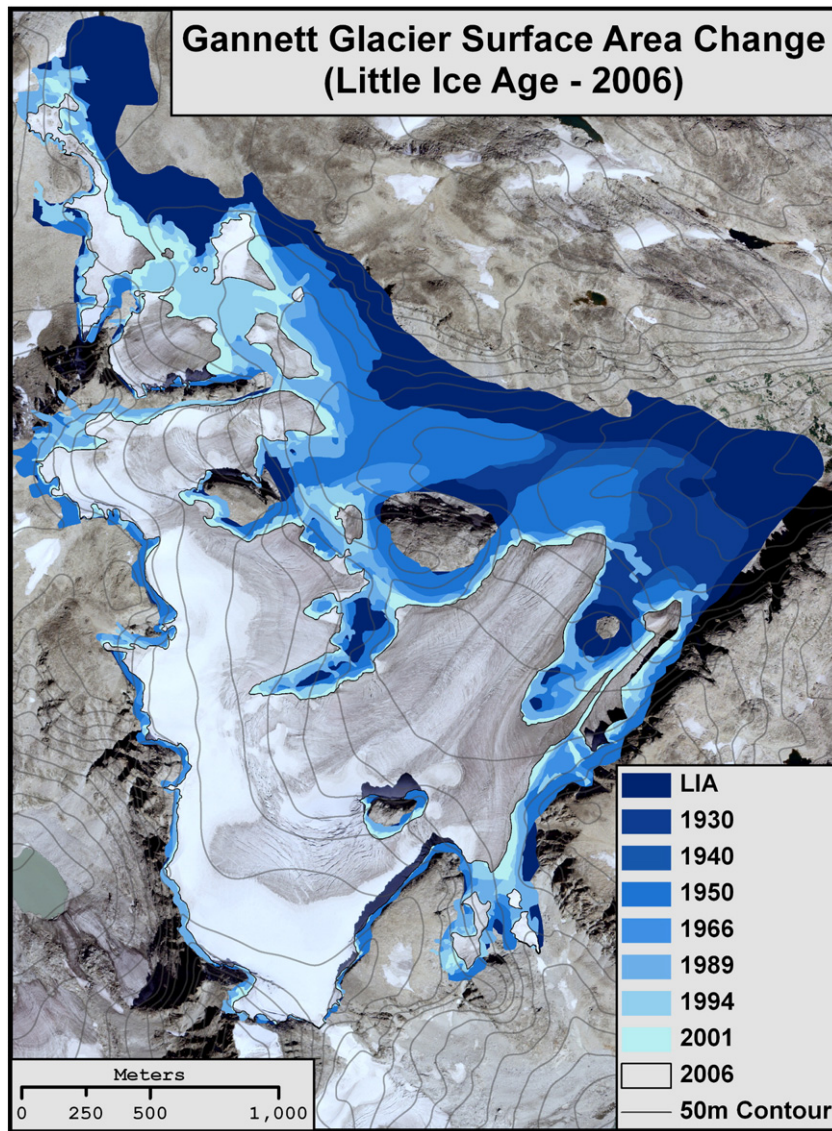


Fig. 9. Surface area change of Gannett Glacier from the end of the LIA (~1900) to 2006 mapped on a 2006 NAIP color DOQ.

correlation analysis underscoring the importance of elevation to glacier change and that glaciers at lower elevations recede more than at upper elevations. Air temperature was also shown to be significant in both analyses, but with minimum temperatures rather than maximum temperatures in the correlation analysis. Spring and autumn temperatures were significant variables in both analyses.

4.3. Ice mass wastage contribution to runoff

The four gauged watersheds vary in area and G&PS cover, and no watershed exceeds 7% ice cover (Fig. 4, Table 7). The range of G&PS volume change was used to estimate August and September meltwater runoff for each watershed (Table 8). Dinwoody Creek had the greatest average contribution of meltwater, with an estimated range of 4.4–14.1%. Pine Creek had the lowest average runoff contribution, with an estimated range of 0.6–1.9%. The relative contribution of meltwater to stream runoff within each watershed

was consistent with the fractional area covered by ice. For the three largest watersheds, the time period with the greatest contribution of G&PS melt to stream runoff was 1994 to 2001, with an estimated contribution to Dinwoody Creek alone ranging from 7.1 to 22.6%.

5. Discussion and conclusions

When the U.S. Geological Survey mapped the Wind River Range at 1:24,000, they identified 679 snow and ice features of which at least 269 are G&PS covering $46.96 \pm 0.12 \text{ km}^2$ and do not exceed 428 G&PS covering a total area of $50.51 \pm 0.13 \text{ km}^2$. The range in these numbers is from the ambiguity in defining and tracking the 159 features excluded because of late season snowfall or shadows within the imagery. The 269 G&PS are typically small, averaging 0.175 km^2 (median 0.037 km^2) with an average elevation of 3651 m and ranging from 3239 m to 4153 m. Of these 269 G&PS, 43 were identified as glaciers based on estimates of their basal shear stress,

corresponding to a count of 44 glaciers nominally identified as the primary group (Thompson et al., 2011). We have likely underestimated the number of glaciers. Our estimate of G&PS change between 1966 and 2006, –26%, is similar to that of Edmunds et al.'s (2011) –25% between 1967 and 2006 in the neighboring Teton Range, and a bit larger than the change of the 14 Meier glaciers, –20%, in the Wind River Range. But our results are much smaller than those of Thompson et al. (2011), –38%, in the Wind River Range over the same period. Although our sample size differs greatly, 217 G&PS versus 44 glaciers, it's unlikely that sample size alone explains the difference. The difference may be attributable to the data source for the 1966 inventory. We used the USGS quadrangle outlines, whereas Thompson et al. (2011) reinterpreted the original aerial imagery. For the period ~1950 to 2001, the 14 Meier glaciers shrank about 27% compared to 15% in the Canadian Rockies (DeBeer and Sharp, 2007). Between the end of the LIA, ~1900, and 2006 our results showed that the glacier area decreased from about 62.3 to 32.8 km², a loss of about 47%, with the largest glacier, Gannett, shrinking by 2.44 km² during this time (Fig. 9). The magnitude of change in the Wind River Range is consistent with that observed elsewhere in the continental U.S., including the Sierra Nevada –55% (Basagic and Fountain, 2011) and the Colorado Front Range about –34% (Hoffman et al., 2007), and elsewhere globally (e.g., Paul et al., 2004). The rate of glacier change over the past century is consistent with glaciers elsewhere in the U.S. and in the Northern Hemisphere with rapid shrinkage after the Little Ice Age, from ~1900, through to about the 1950s, after which the shrinkage generally slowed and in some cases glaciers enlarged. By the early 1990s, the glaciers resumed their rapid shrinkage. No glaciers disappeared since 1966 that we can detect. This is consistent with the results of Granshaw and Fountain (2006) who found that in the Cascade Mountains of Washington less than five G&PS disappeared between 1958 and 1998.

Most glacier inventories set a minimum area criterion, typically 0.1 km², below which features are ignored (e.g., Post, 1971; Paul et al., 2004). The advantage of this approach is its simplicity and it eliminates many seasonal features; however, it also eliminates an unknown number of perennial features. Our approach attempts to define perennial by examining features over time. We are interested in the hydrologic contribution of all perennial features that may be important to small alpine watersheds as well as their collective influence on regional runoff. Our inventory can be made compatible to the conventional ones simply by imposing a minimum size criterion.

The attempt to include data from other authors highlights the difficulty and potentially large errors incurred. Quality control and assumptions differ between studies. If all protocols are identical, different investigators commonly define a glacier perimeter differently. For example, some investigators may include a small tributary ice patch while others may exclude it (e.g., Jackson and Fountain, 2007). Combining these two data sets without regard to understanding differing assumptions and techniques, particularly as sequential time series, leads to erroneous results. This issue becomes particularly important when a glacier ablates into separate ice bodies. In any case, this circumstance underscores the importance for closely examining the source of area data gleaned from the literature or from other investigators.

The correlation analysis identified elevation and air temperatures explaining most of the variability in P&GS area change, and the PCA analysis suggested that they account for 38% of the variability between glaciers. Elevation is not a driver of change per se but sets the environment and, therefore, climatic vulnerability, with G&PS at lower elevations is more vulnerable than the ones at higher elevations. Lower elevations are warmer, receive less snow, and increasingly, frequent winter rain events (McCabe et al., 2007), yielding shorter winters and less snow accumulation (McCabe and

Fountain, 1995). The northern Rocky Mountains, including the Wind River Range, have been subjected to these elevational effects on snow cover, and lower elevation snowpacks have thinned over time compared to those at high elevations (Hall et al., 2012; Pederson et al., 2013). Furthermore, elevation should be a more sensitive indicator compared to air temperature in our analysis because our elevation data have a spatial resolution of 10 m, whereas air temperature has a spatial resolution of 4 km. Within that 4-km cell, a number of different G&PS maybe be present but at differing elevations. The identification of spring and autumn air temperature in the correlation and PCA analysis suggests the emerging importance of warmer air temperatures in these seasons, which lengthen the ablation season. The importance of spring temperatures was found in the Colorado Front Range (Hoffman et al., 2007) and in the Sierra Nevada (Basagic and Fountain, 2011). Declining snowpack over the past few decades is directly related to spring temperatures (Pederson et al., 2013). The importance of warming winter temperatures was indicated only in the correlation analysis using the full 217 G&PS data set and not in the 14-glacier data set or in the PCA. This may be an effect of elevation and the influence of the low elevation glaciers. Surprisingly, correlations with summer air temperatures were not significant and we infer the variability in the winter (and perhaps spring and autumn) temperatures to be the more influential factors. Precipitation was not significantly correlated with G&PS change over time but is identified as a significant factor in the PCA (~23%). This likely indicates a strong spatial variation accounting for the variance. The G&PS that receive less precipitation are more vulnerable to variations in air temperature and shrinkage. Finer spatial resolution data on temperature and precipitation data will be needed to adequately examine the relationship between glacier change and local environment, a particular issue in mountainous regions where avalanching and wind drift play vital roles for small glaciers (Kuhn, 1995). We infer from these correlations and from the PCA analyses that the G&PS at low elevations are shrinking faster than those at higher elevations and that the principle driver is warming air temperatures.

The loss of long-term storage and subsequent contribution of meltwater to late summer stream runoff is significant. The two watersheds with glacier cover exceeding 2% are of particular concern, with total percent contributions ranging from 2 to 6% and from 4 to 14%, and in one eight-year period ranging as high as 3–10% and 7–22%. These results are consistent with those of Bell et al. (2012) who found that total glacial runoff, which included loss from long-term and seasonal storage, accounted for 23–54% of the total runoff from the watershed. Furthermore, our results are consistent with Thompson (2009) and Marks (2012) who estimated that the loss from long-term storage accounted for 2–12% of the late summer runoff. The anticipated shrinkage of glaciers with continued climate warming will increase the drought stress of these watersheds directly through the loss of runoff and indirectly by increased water loss through evaporation.

Acknowledgments

The authors would like to thank Dr. Richard Marston (editor) and the four anonymous reviewers for their constructive comments during the review and revision process. In addition, we would like to thank Kristina Dick and Kat Armstrong for helping with data preparation; Dr. Bruce Pigozzi for general statistics advice; and last but not least, Dr. Mark F. Meier for his contributions to this study and glaciology as a whole. This research was supported by a Portland State University Scholarly and Creative Activity Grant for Undergraduates, and by the U.S. Geological Survey.

Appendix A

Table A1
Predicted surface area change and topographic/climate variable relationship and correlation analysis results; significant one-tail results are in bold; results significant with a two-tail test are italicized; however, these results are considered spurious since they do not correspond with the predicted relationship.

Variable	Predicted relationship	1900 to 1966	1900 to 1994	1900 to 2001	1900 to 2006	1966 to 1994		1966 to 2001		1966 to 2006		1994 to 2001		1994 to 2006		2001 to 2006	
		Glacier subset	Glacier subset	Glacier subset	Glacier subset	Perennial features	Glacier subset										
Longitude	-	-0.040	0.078	0.043	-0.048	-0.031	0.163	<i>0.185</i>	0.063	0.110	-0.066	<i>0.236</i>	-0.145	0.120	-0.310	-0.091	-0.388
Latitude	+	0.163	0.025	0.091	0.163	-0.087	-0.177	<i>-0.186</i>	-0.011	<i>-0.160</i>	0.101	-0.132	0.274	-0.020	0.391	0.059	0.375
Minimum elevation	+	0.237	0.393	0.375	0.317	0.496	0.272	0.214	0.210	0.266	0.150	<i>-0.183</i>	-0.026	<i>-0.318</i>	-0.077	-0.045	-0.117
Maximum elevation	+	0.444	0.577	0.660	0.725	0.365	0.276	0.499	0.408	0.332	0.532	0.207	0.386	<i>-0.149</i>	0.580	<i>-0.279</i>	0.552
Mean elevation	+	0.370	0.643	0.735	0.736	0.513	0.490	0.411	0.579	0.345	0.606	-0.004	0.392	<i>-0.291</i>	0.451	<i>-0.184</i>	0.305
Northness	+	0.041	0.227	0.184	0.170	0.063	0.289	-0.036	0.172	-0.021	0.143	-0.111	-0.115	-0.123	-0.077	0.075	0.001
Eastness	+	0.218	0.138	0.108	0.087	0.071	-0.086	0.069	-0.071	0.013	-0.076	0.002	-0.002	-0.122	-0.017	-0.046	-0.022
Min autumn temp	-	-0.193	-0.298	-0.287	-0.249	0.070	-0.117	-0.036	0.043	-0.094	0.071	-0.006	0.271	0.042	0.230	0.041	0.070
Min spring temp	-	-0.235	-0.307	-0.265	-0.290	0.112	-0.117	0.072	-0.040	0.013	-0.110	0.018	-0.045	0.121	-0.180	0.057	-0.275
Min summer temp	-	-0.241	-0.340	-0.319	-0.312	-0.029	-0.236	-0.060	-0.131	-0.064	-0.141	0.030	-0.007	0.126	-0.110	0.067	-0.194
Max autumn temp	-	-0.209	-0.165	-0.193	-0.296	-0.173	0.011	-0.016	-0.089	-0.070	-0.248	0.140	-0.180	<i>0.217</i>	-0.407	0.030	-0.434
Max winter temp	-	-0.265	-0.273	-0.278	-0.331	-0.352	-0.160	-0.249	-0.133	-0.260	-0.235	0.057	0.161	<i>0.245</i>	-0.197	0.048	-0.465
Max spring temp	-	-0.204	-0.271	-0.207	-0.273	-0.302	-0.161	-0.176	-0.081	-0.223	-0.201	0.105	0.035	<i>0.235</i>	-0.249	0.015	-0.424
Max summer temp	-	-0.202	-0.300	-0.228	-0.277	-0.316	-0.226	-0.218	-0.117	-0.249	-0.224	0.079	0.041	<i>0.239</i>	-0.291	0.036	-0.522
Autumn precipitation	+	-0.048	0.024	-0.026	0.032	0.236	0.106	0.096	0.022	0.136	0.112	-0.041	0.005	<i>-0.175</i>	0.090	-0.032	0.061
Winter precipitation	+	-0.028	-0.017	-0.068	-0.012	0.208	0.061	0.032	-0.017	0.089	0.065	<i>-0.173</i>	-0.165	<i>-0.162</i>	-0.016	0.024	0.147
Spring precipitation	+	-0.100	-0.028	-0.061	0.019	0.212	0.084	0.060	-0.003	0.092	0.128	<i>-0.138</i>	-0.038	<i>-0.204</i>	0.299	0.012	0.418
Summer precipitation	+	-0.035	0.047	-0.019	0.053	0.166	0.075	0.002	-0.005	0.034	0.105	<i>-0.161</i>	-0.053	-0.124	0.334	0.027	0.448

Table A2
List of USGS 1:24,000 topographic maps, Wind River Range, Wyoming, used to identify the baseline coverage of perennial snow and ice features^a.

Quad name	USGS Quad ID	Photo date	# of features	Total area (km ²)	% U	Largest feature (km ²)	Min elevation (m)	Max elevation (m)
Gannett Peak	43109-B6	1966	105	18.66	0.40	3.32	3315	4206
Downs Mountain	43109-C6	1966	106	9.51	0.56	2.50	3220	4029
Fremont Peak North	43109-B5	1966	41	8.89	0.58	2.79	3399	4174
Fremont Peak South	43109-A5	1966	61	5.46	0.74	1.36	3353	4115
Simpson Lake	43109-D6	1966	19	2.64	1.06	0.94	3182	3739
Roberts Mountain	42109-H3	1974	69	2.51	1.09	0.20	3181	3865
Halls Mountain	42109-H4	1974	100	1.74	1.31	0.15	3209	3687
Lizard Head Peak	42109-G2	1974	48	1.73	1.31	0.28	3114	3798
Mount Bonneville	42109-G3	1974	53	1.04	1.70	0.09	3177	3785
Temple Peak	42109-F2	1968	19	1.02	1.71	0.27	3268	3924
Union Peak	43109-D7	1966	29	0.87	1.85	0.16	3151	3515
Ink Wells	43109-C5	1966	9	0.25	3.44	0.07	3270	3694
Green River Lakes	43109-C7	1966	8	0.11	5.19	0.03	3295	3607
Squaretop Mountain	43109-B7	1966	9	0.09	5.74	0.02	3276	3540
Horseshoe Lake	42109-H5	1963	2	0.05	8.05	0.03	3362	3520
Washakie Park	42109-H2	1974	1	0.04	9.06	0.04	3251	3368
Total			679	54.59	0.23	3.32	3114	4206

^a The table is sorted by the total ice-covered area within each quadrangle. % U is the percent total uncertainty of the total surface area of perennial snow and ice features. Total uncertainty is calculated by taking the root of the sum of squared uncertainty of each feature in a quadrangle map. Max/min elevation is the centroid elevation of the highest, lowest feature within the quadrangle. Aerial photo year is the date the aerial photography was acquired from which the USGS map was derived.

References

- Badescu, V., Zamfir, E., 1999. Degree-days, degree-hours and ambient temperature bin data from monthly-average temperatures (Romania). *Energy Convers. Manag.* 40, 885–900.
- Bahr, D.B., Meier, M.F., Peckham, S.D., 1997. The physical basis of glacier volume–area scaling. *J. Geophys. Res.* 102, 20355–20362.
- Barnett, T.P., Adam, J.C., Lettenmaier, D.P., 2005. Potential impacts of a warming climate on water availability in snow-dominated regions. *Nature* 438, 303–309.
- Basagic, H.J., Fountain, A.G., 2011. Quantifying 20th century glacier change in the Sierra Nevada, California. *Arct. Antarct. Alp. Res.* 43, 317–330.
- Bell, J., Tootle, G., Pochop, L., Kerr, G., Sivanpillai, R., 2012. Glacier impacts on summer streamflow in the Wind River Range, Wyoming. *J. Hydrol. Eng.* 17, 521–527.
- Boe, B.A., 2008. Operational aspects of the Wyoming weather modification pilot project—an update.
- Cheesbrough, K.S., 2007. *Glacial Recession in Wyoming's Wind River Range*. University of Wyoming, Laramie, WY.
- Chen, J., Ohmura, A., 1990. Estimation of Alpine glacier water resources and their change since the 1870s. *Proceedings of the Two Lausanne Symposia*. Presented at the Hydrology in Mountainous Regions — I. Hydrologic Measurements, the Water Cycle. International Association of Hydrological Sciences, pp. 127–135.
- Cuffey, K.M., Paterson, W.S.B., 2010. *The Physics of Glaciers*, 4th ed. Academic Press.
- Daly, C., Taylor, G.H., Gibson, W.P., 1997. The PRISM approach to mapping precipitation and temperature. Presented at the 10th Conference on Applied Climatology, American Meteorology Society, Reno, NV, pp. 10–12.
- DeBeer, C.M., Sharp, M.J., 2007. Recent changes in glacier area and volume within the southern Canadian Cordillera. *Ann. Glaciol.* 46, 215–221.
- Delo, D.M., 1940. Recent recession of Dinwoody glaciers, Wind River Mountains, Wyoming. *Geological Society of America Bulletin* 51.
- Dyrgerov, Mark B., Meier, Mark F., 2000. Twentieth century climate change: evidence from small glaciers. *Proc. Natl. Acad. Sci.* 97, 1406–1411.
- Edmunds, J., Tootle, G., Kerr, G., Sivanpillai, R., Pochop, L., 2011. Glacier variability (1967–2006) in the Teton Range, Wyoming, United States. *J. Am. Water Resour. Assoc.* 48, 187–196.
- Fountain, A.G., Tangborn, W.V., 1985. The effect of glaciers on streamflow variations. *Water Resour. Res.* 21, 579–586.
- Fountain, A.G., Hoffman, M.J., Jackson, K.M., Basagic, H.J., Nysten, T.H., Percy, D., 2007. Digital outlines and topography of the glaciers of the American West. Open-File Report No. 2006-1340. U.S. Geological Survey.
- Chilani, C.D., 2000. Demystifying area uncertainty: more or less. *Surveying and Land Information Systems* 60, pp. 177–182.
- Gong, P., Zheng, X., Chen, J., 1995. Boundary uncertainties in digitized maps: an experiment on digitization errors. *Geogr. Inf. Sci.* 1, 65–72.
- Granshaw, F.D., Fountain, A.G., 2006. Glacier change (1958–1998) in the North Cascades National Park Complex, Washington, USA. *J. Glaciol.* 52, 251–256.
- Hall, D.K., Foster, J.L., DiGirolamo, N.E., Riggs, G.A., 2012. Snow cover, snowmelt timing and stream power in the Wind River Range, Wyoming. *Geomorphology* 137, 87–93.
- Hayden, F.V., 1878. Discovery of recent glaciers in Wyoming. *Am. Nat.* 12, 827–833.
- Hayden, F.V., 1879. Eleventh Annual Report of the United States Geological and Geographical Survey of the Territories; Embracing Idaho and Wyoming, Being a Report of the Progress of the Exploration for the Year 1877. Government Printing Office, Washington D.C.
- Hayden, F.V., 1883. 12th Annual Report of the United States Geological and Geographical Survey of the Territories: A report of the progress of the exploration in Wyoming and Idaho for the year 1878.
- Hoffman, M.J., Fountain, A.G., Achuff, J.M., 2007. 20th-century variations in area of cirque glaciers and glacierets, Rocky Mountain National Park, Rocky Mountains, Colorado, USA. *Ann. Glaciol.* 46, 349–354.
- Hughes, M.L., McDowell, P.F., Marcus, W.A., 2006. Accuracy assessment of georectified aerial photographs: implications for measuring lateral channel movement in a GIS. *Geomorphology* 74, 1–16.
- Jackson, K.M., Fountain, A.G., 2007. Spatial and morphological change on Eliot Glacier, Mount Hood, Oregon, USA. *Ann. Glaciol.* 46, 222–226.
- Jansson, P., Hock, R., Schneider, T., 2003. The concept of glacier storage: a review. *J. Hydrol.* 282, 116–129.
- Kaser, G., Cogley, J.G., Dyurgerov, M.B., Meier, M.F., Ohmura, A., 2006. Mass balance of glaciers and ice caps: consensus estimates for 1961–2004. *Geophys. Res. Lett.* 33, L19501.
- Kuhn, Michael, 1995. The mass balance of very small glaciers. *Z. Gletscherk. Glazialgeol.* 5, 171–179.
- LaChapelle, E.R., 1965. The mass budget of Blue Glacier, Washington. *J. Glaciol.* 5, 609–623.
- Maidment, D.R., 2002. *ArchHydro: GIS for Water Resources*. ESRI Inc., Redlands, CA.
- Marks, J.A., 2012. *Estimates of Glacier Mass Loss and Contribution to Streamflow: Wind River Range (Wyoming, USA)*(M.S. Thesis) University of Tennessee, (40 pp.).
- Marston, R.A., Pochop, L.O., Kerr, G.L., Varuska, M.L., 1989. Recent trends in glaciers and glacier runoff, Wind River Range, Wyoming. Presented at the Proceedings of the Symposium on Headwaters Hydrology. American Water Resources Association, Bethesda, MD.
- Marston, R.A., Pochop, L.O., Kerr, G.L., Varuska, M.L., 1991. Recent glacier changes in the Wind River Range, Wyoming. *Phys. Geogr.* 12, 114–123.
- McCabe, G.J., Fountain, A.G., 1995. Relations between atmospheric circulation and mass balance of South Cascade Glacier, Washington, USA. *Arct. Alp. Res.* 27, 226–233.
- McCabe, G.J., Clark, M.P., Hay, L.E., 2007. Rain-on-snow events in the western United States. *Bull. Am. Meteorol. Soc.* 88, 319–328.
- Meier, M.F., 1951. *Glaciers of the Gannett Peak-Fremont Peak Area*. State University of Iowa, Wyoming.
- Middelkoop, H., 1990. Uncertainty in a GIS: a test for quantifying interpretation output. *Int. J. Appl. Earth Obs. Geoinf.* 225–232.
- Moore, R.D., Fleming, S.W., Menounos, B., Wheate, R., Fountain, A., Stahl, K., Holm, K., Jakob, M., 2009. Glacier change in western North America: influences on hydrology, geomorphic hazards and water quality. *Hydrol. Process.* 23, 42–61.
- Paul, F., Kääb, A., Maisch, M., Kellenberger, T., Haeberli, W., 2004. Rapid disintegration of Alpine glaciers observed with satellite data. *Geophys. Res. Lett.* 31, L21402.
- Pederson, Gregory T., Betancourt, Julio L., McCabe, Gregory J., 2013. Regional patterns and proximal causes of the recent snowpack decline in the Rocky Mountains. *U.S. Geophysical Research Letters* 40, pp. 1811–1816.
- Pfeffer, W.T., Harper, J.T., O'Neel, S., 2008. Kinematic constraints on glacier contributions to 21st-century sea-level rise. *Science* 321, 1340.
- Pochop, L.O., Marston, R.A., Kerr, G.L., Varuska, M.L., 1989. Long-term Trends in Glacier and Snowmelt Runoff Wind River Range, Wyoming (Project Report). Wyoming Water Research Center, University of Wyoming, Laramie, WY.
- Pochop, L., Marston, R., Kerr, G., Veryzer, D., Varuska, M., Jacobel, R., 1990. Glacial icemelt in the Wind River Range, Wyoming. Presented at the Watershed Planning and Analysis in Action. American Society of Civil Engineers, Durango, CO, pp. 118–124.
- Post, A., 1971. *Inventory of Glaciers in the North Cascades*, Washington. US Government Printing Office, Washington D.C.
- Russell, I.C., 1885. *Existing Glaciers of the United States*. Department of the Interior; U.S. Geological Survey.
- Sitts, D.J., Fountain, A.G., Hoffman, M.J., 2010. Twentieth century glacier change on Mount Adams, Washington, USA. *Northwest Sci.* 84, 378–385.
- Sprague, M., 1964. *The Great Gates: The Story of the Rocky Mountain Passes*. Little, Brown, and Company, Boston, MA.
- Thompson, D., 2009. *Glacier Variability in the Wind River Range, Wyoming, U.S.A.*(M.S. thesis) Department of Civil and Architectural Engineering, Univ. of Wyoming, Laramie, WY.
- Thompson, D., Tootle, G., Kerr, G., Sivanpillai, R., Pochop, L., 2011. Glacier variability in the Wind River Range, Wyoming. *J. Hydrol. Eng.* 16, 798–805.
- VanLooy, J.A., Miede, C., Vandeberg, G.S., Forster, R.R., 2014. Ice volume estimation inferred from ice thickness and surface measurements for continental glacier, Wind River Range, Wyoming, USA. *J. Glaciol.* 60, 478–488.
- Wang, T., Hamann, A., Spittlehouse, D.L., Aitken, S.N., 2006. Development of scale-free climate data for Western Canada for use in resource management. *Int. J. Climatol.* 26, 383–397.
- Wentworth, C.K., Delo, D.M., 1931. Dinwoody glaciers, Wind River Mountains, Wyoming; with a brief survey of existing glaciers in the United States. *Bull. Geol. Soc. Am.* 42, 605–620.
- Wilson, H.M., 1907. Topographic surveys in the United States. *Bull. Am. Geogr. Soc.* 39, 13–24.
- Wolken, G.J., 2000. *Energy Balance and Spatial Distribution of Net Radiation on Dinwoody Glacier, Wind River Range, Wyoming, USA*(Masters Thesis) University of Wyoming.